Angewandte Chemie
Eine Zeitschrift der Gesellschaft Deutscher Chemiker

Supporting Information

Transfer of Axial Chirality to the Nanoscale Endows Carbon Nanodots with Circularly Polarized Luminescence

S. Di Noja, F. Amato, F. Zinna, L. Di Bari, G. Ragazzon*, M. Prato**

SUPPORTING INFORMATION

Table of Contents

Experimental Procedures

A. General information

Microwave synthesis was performed on a CEM Discover-SP, using 10 mL glass microwave vials. The synthetic protocols could be reproduced also on an Anton Paar 400 microwave reactor. NMR spectra were recorded on Varian 400 spectrometer (^{1}H: 400 MHz). UV-Vis measurements were carried out on PerkinElmer Lambda 35 UV-Vis spectrophotometer. All the spectra were recorded at room temperature using 10 mm path-length cuvettes. Atomic force microscopy (AFM) images were obtained with a Nanoscope IIIa, VEECO Instruments. As a general procedure, AFM analyses were performed using tapping mode with a HQ:NSC19/ALBS probe (80 kHz; 0.6 N/m) (MikroMasch) from drop cast of samples in ethyl acetate diluted solution (concentration in the order of µg/mL) on an exfoliated mica substrate. The obtained AFM images were analyzed in S3 Gwyddion 2.58, using Profile extraction tool and Find peaks function. Statistical analysis was carried out on one hundred nanoparticles. TEM images were acquired on Jeol, JEM 2100, Japan, at 200 kV. The TEM is equipped with Gatan camera and DigitalMicrographs software. Samples were drop cast from an ethyl acetate diluted solution (concentration in the order of µg/mL) on top of a copper grid (copper-grid-supported carbon film), purchased from Ted Pella, Inc. Finally, the solvent was removed in vacuum. ATR-Fourier-transform infrared spectroscopy was performed on a Shimadzu IRAffinity-1S equipped with a QATR-10 with diamond crystal. Typically, spectra were recorded with 4 cm-1 resolution and 60 scans accumulation. Electronic Circular Dichroism (ECD) spectra were recorded using Jasco J-810 at room temperature (20 °C). Conditions were as follows: scanning rate 100 nm/min, data pitch 1 nm, Digital Integration Time (D.I.T.) 2 s, 3 accumulations. Luminescence lifetimes were measured with an Edinburgh Instruments FS5 time-correlated single-photon counting spectrofluorimeter, exciting the sample at 375 nm with a picosecond pulsed diode laser (EPL-375 Edimburgh Instruments).

For thin layer chromatography (TLC) analysis, Merck pre-coated TLC plates (silica gel 60 GF254, 0.25 mm) were employed, using UV light as the visualizing agent (254 nm). For filtration, Merck Omnipore 0.1 µm PTFE Membrane filters (25 mm) were employed. Organic solutions were concentrated under reduced pressure on a Büchi rotatory evaporator. X-Ray Photoelectron Spectroscopy experiments were performed on a SPECS Sage HR 100 spectrometer with a non-monochromatized X ray source (Magnesium Kα line of 1253.6 eV energy and 252 W), placed perpendicular to the analyzer axis and calibrated using the 3d5/2 line of Ag with a full width at half maximum (FWHM) of 1.1 eV. The selected resolution for the spectra was 15 eV of Pass Energy and 0.15 eV/step. All measurements were made in an ultra-high vacuum (UHV) chamber at a pressure around 8·10-8 mbar. Samples were prepared drop casting a dispersion of the samples in chloroform on gold slides prepared in house and allowing to dry overnight. CasaXPS software (version 2.3.16 PR1.6) was used for data analysis. Survey spectra were employed to calculate relative atomic composition of all elements present in the samples. General procedures and materials. Carbon Nanodots (CNDs) were synthesized in glass microwave vials. Commercial reagents and solvents were used as purchased from Sigma-Aldrich or VWR and used as received, without further purification, unless otherwise stated. Citric acid, (*S*)-1,1'-binaphthyl-2,2'-diamine, (*R*)-1,1'-binaphthyl-2,2'-diamine and 1,4-benzoquinone are all commercially available. Quantum yield (QY) measurements were performed with quinine sulphate in 0.10 M H_2SO_4 (literature quantum yield 0.54 at 360 nm) [1] as standard and CNDs-*S*-2 or CNDs-*R*-2 in $CHCl_3$ solution. The fluorescence quantum yields were calculated according to the Equation 1

$$\Phi_x = \Phi_{st} \frac{I_x}{I_{st}} \frac{A_{st}}{A_x} \frac{n_x^2}{n_{st}^2}$$

I is the measured integrated fluorescence emission intensity. *A* is the absorbance value, *n* is the refractive index of the solvent and *Φ* is the quantum yield. The index *x* is referred to the sample, and the index *st* is referred to the standard. The absorbance of the standard and the sample were measured with A<0.1 at the excitation wavelength. The quantum yield was calculated at different excitation wavelengths by taking advantage of the following proportion:

$$\Phi_{exc} \propto \frac{I_{exc}}{A_{exc}}$$

Where the subscript *exc* indicates a specific excitation wavelength. The estimated experimental error on QY is 25%.

CPL measurements were carried out with a home-made spectrofluoropolarimeter.[2] In the current configuration the setup is optimized for visible measurements (400-750 nm), while efficient measurements in the UV region are out of range, due to emission monochromator grating efficiency. This experimental limitation prevented the observation of CPL from **CNDs-1** which may also be CPL-active. The samples were dissolved in CH_2Cl_2 and displayed absorbance 0.25 at 420 nm. A 365 nm LED was used as the excitation source, employing a 90° geometry. The excitation light was linearly polarized parallel to the detection direction. Acquisition parameters were: band-with ~10 nm, scan-speed 1 nm/sec, integration time 8 sec, photomultiplier voltage 600 V, accumulations 20 for spectra in CH_2Cl_2 and 10 for spectra in DMF.

$CHCl_3$ was employed in the optical characterization because of its ease of processing (lower boiling point) and UV-cutoff at shorter wavelengths with respect to DMF. This allowed also consistency with NMR characterization, performed in $CDCl_3$. The CPL measurements were performed in DCM, which offers a low viscosity, beneficial in increasing the tumbling rate of the molecules therefore minimizing photoselection. Photoselection may indeed affect measurements since the rotational correlation time (estimated being 2 to 3 ns on the basis of their size) in $CHCl_2$ is similar to recorded luminescence lifetime (2.7 ns for **CNDs-2**, *vide infra*, Fig. S31,32 and Table S6). Anyway, we note that even a much polar and completely different solvent such as DMF gives similar CPL spectra (*vide infra*, Fig S26), indicating that the solvent nature does not significantly change the CPL response.

B. Synthesis of Carbon Nanodots

CNDs-*S*-1 and CNDs-*R*-1 (CNDs-1)

Either (*S*)- or (*R*)-1,1'-binaphthyl-2,2'-diamine (75 mg, 0.264 mmol, 1 eq.) and citric acid (76 mg, 0.396 mmol, 1.5 eq.) were dissolved in N,N-dimethylformamide (DMF) (250 µL) and then heated at 240° C, 80 psi and 200 W for 300 seconds. In the process of microwave heating, the solution changes color from pale pink to brown as a result of formation of CNDs-2. The solution was diluted with DMF and filtered through a 0.1 µm microporous membrane to remove possible large aggregates. The solution was collected and 50 mL of cold diethyl ether (Et_2O) were added in order to induce CNDs' precipitation. The precipitate was filtered through a 0.1 µm microporous membrane and washed with 50 mL of Et_2O, giving a pale pink powder (CNDs-*S*-1: 18 mg, CNDs-*R*-1: 17 mg).

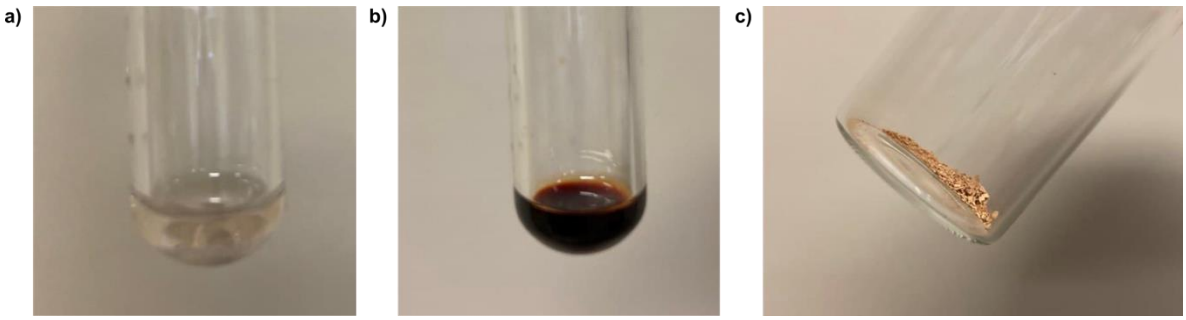

Figure S1. Photographs of the vials (a) before and (b) after microwave-heating process and (c) the final **CNDs-1** after precipitation in cold Et_2O and subsequent filtration.

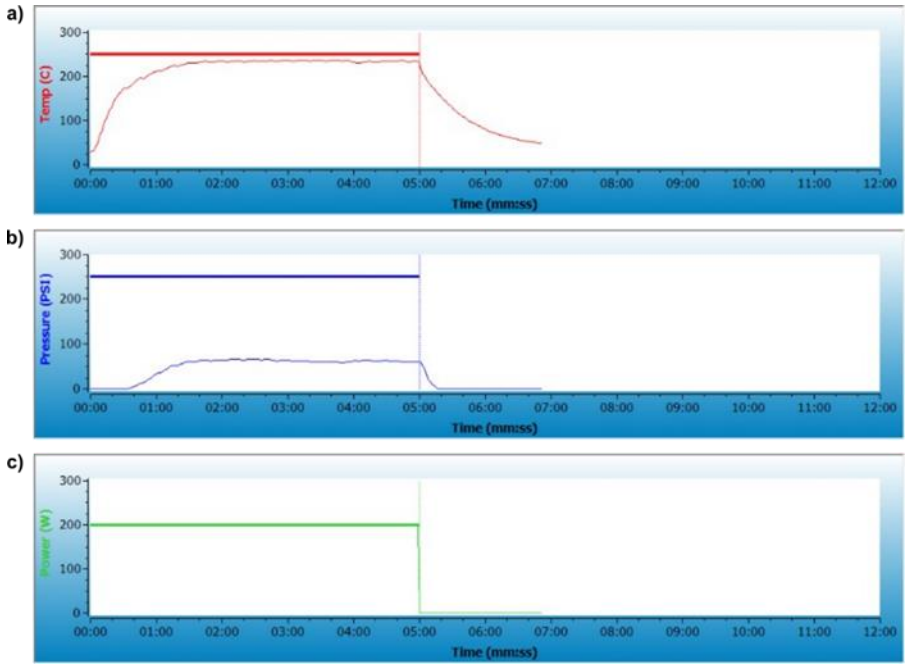

Figure S2. Typical (a) temperature, (b) pressure and (c) power profiles recorded during microwave-heating process for the synthesis of **CNDs-1**.

SUPPORTING INFORMATION

CNDs-*S*-2 and CNDs-*R*-2 (CNDs-2)

Either (*S*)- or (*R*)-1,1'-binaphthyl-2,2'-diamine (75 mg, 0.264 mmol, 1 eq.) and citric acid (76 mg, 0.396 mmol, 1.5 eq.) 1,4-benzoquinone (28.5 mg, 0.264 mmol, 1 eq.) were dissolved in N,N-dimethylformamide (DMF) (250 µL) and then heated at 240° C, 100 psi and 200 W for 300 seconds. In the process of microwave heating, the solution changes color from burgundy to dark brown as a result of formation of CNDs. The solution was diluted with DMF and filtered through a 0.1 µm microporous membrane to remove possible large aggregates. The solution was collected and 50 mL of cold diethyl ether (Et_2O) were added in order to induce CNDs' precipitation. The precipitate was filtered through a 0.1 µm microporous membrane and washed with 50 mL of Et_2O, giving a brown powder (CNDs-*S*: 41 mg, CNDs-*R*: 42 mg). The effective removal of side products is confirmed by TLC. Cyclohexane:ethyl acetate 7:3 or dichloromethane:methanol 95:5 were employed. Using the former eluent, CNDs have an R_f of 0, while other impurities can be identified only in the crude (at higher R_f), but not in the final product. The latter eluent reveals a uniform, broad, stripe with R_f of ca. 0.5. It is possible to solubilize atropoisomeric CNDs in water at spectroscopic concentrations by dissolving them first in DMSO and then adding an aliquot of the obtained solution in water.

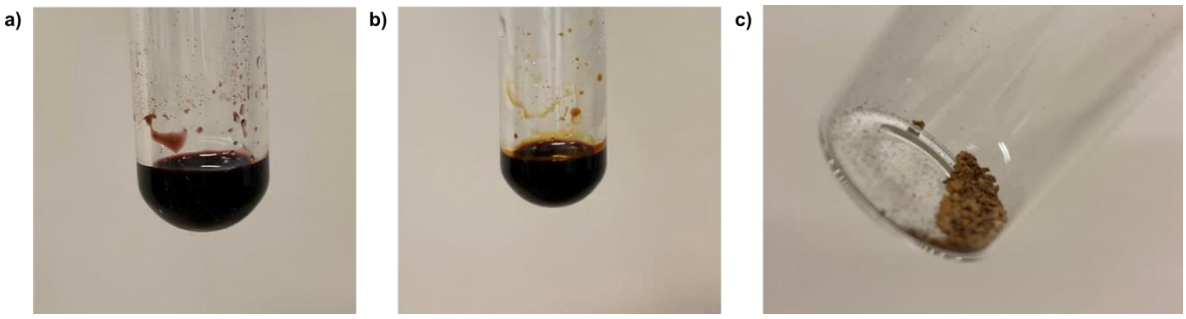

Figure S3. Photographs of the vials (a) before and (b) after microwave-heating process and (c) the final **CNDs-2** after precipitation in cold Et_2O and subsequent filtration.

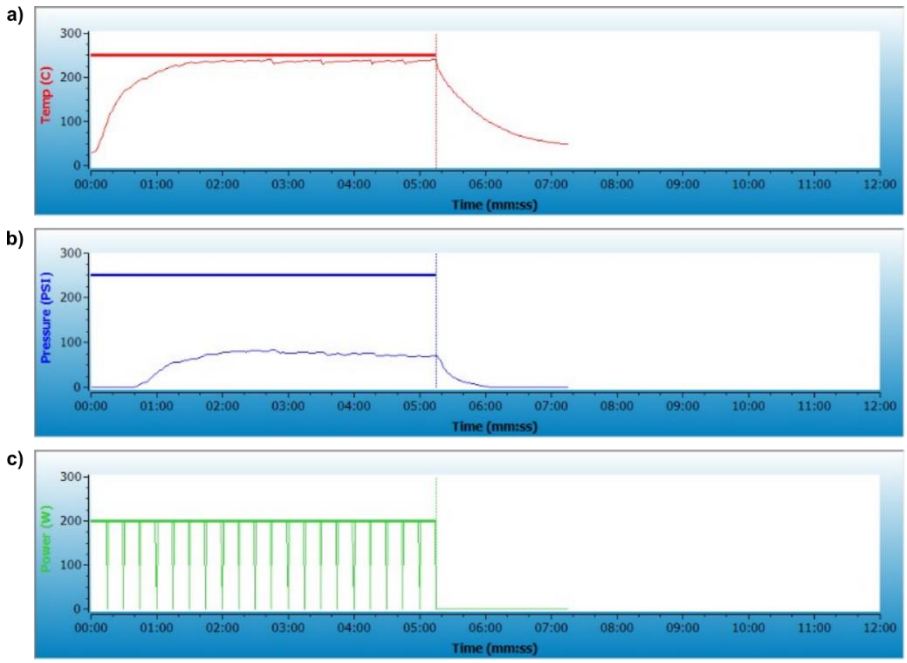

Figure S4. A typical (a) temperature, (b) pressure and (c) power profiles recorded during microwave-heating process for the synthesis of **CNDs-2**.

Results and Discussion

Photophysical and chiroptical characterization of CNDs-1

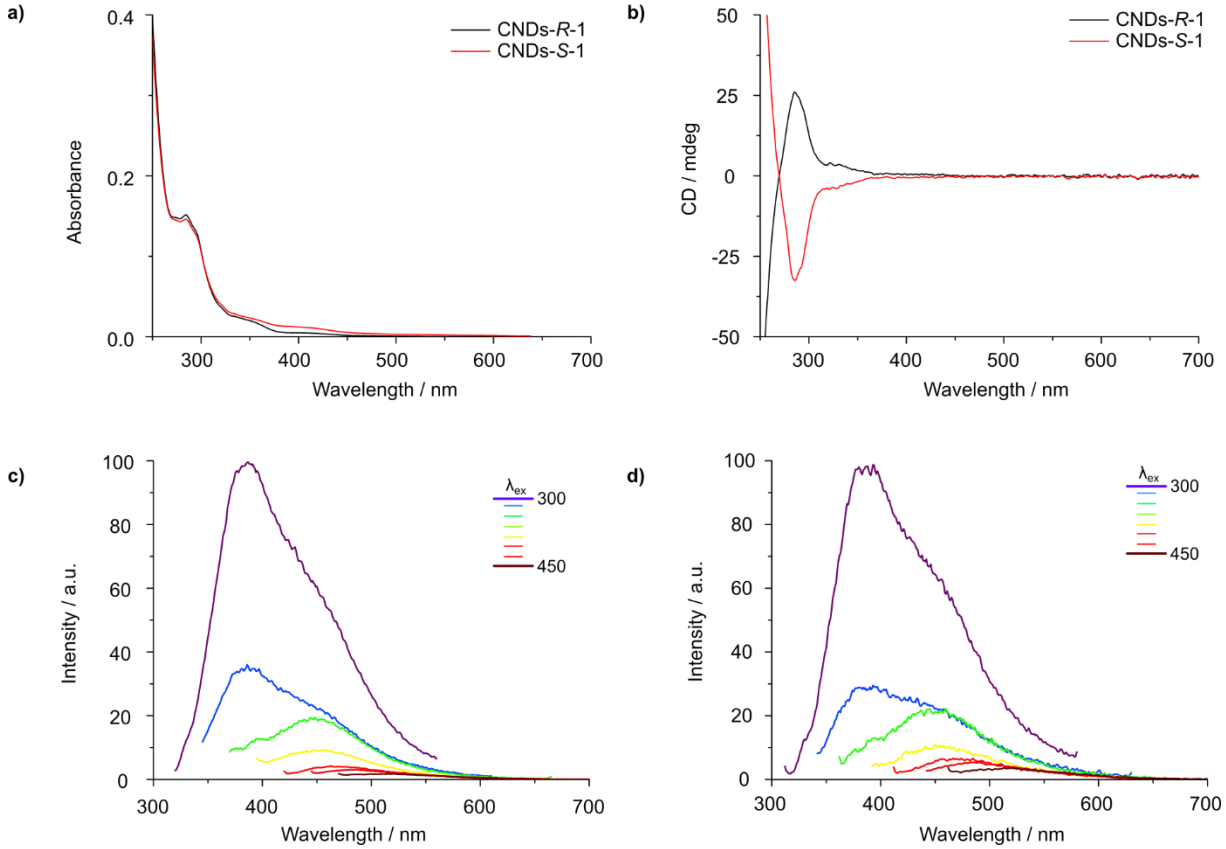

Figure S5. (a) UV-Vis spectra of **CNDs-*R*-1** (black line) and **CNDs-*S*-1** (red line); (b) ECD spectra of **CNDs-*R*-1** (black line) and **CNDs-*S*-1** (red line); (c) and (d) Fluorescence emission spectra of **CNDs-*R*-1** and **CNDs-*S*-1** recorded at different excitation wavelengths. Experiments performed in $CHCl_3$ at r.t., at concentrations between 0.01 and 0.05 mg/mL.

For both **CNDs-1**, at 287 nm, $g_{abs} = |8.0| \times 10^{-4}$. A significantly higher g_{abs} in **CNDs-1** with respect to **CNDs-2** points at g_{abs} values being governed by variations in the dihedral angle of the binaphtyl unit rather than thermal racemization.[3] Indeed, the reaction temperature profiles are very similar for **CNDs-1** and **CNDs-2**. Screening of synthetic parameters also supports the same conclusion, with an increase in **CNDs-2** g_{abs} observed at prolonged reaction times.

Atomic Force Microscopy of CNDs-*R*-1

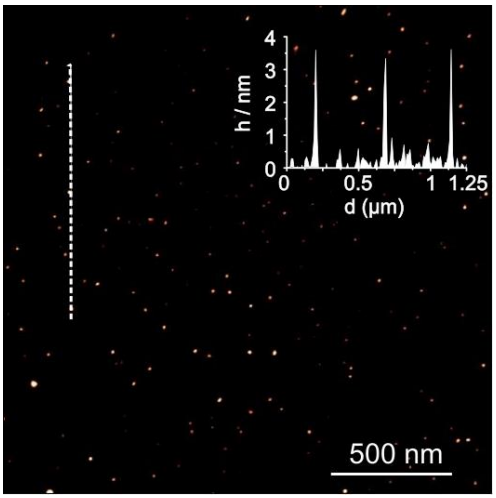

Figure S6. Tapping mode AFM of **CNDs-*R*-1** deposited on a mica substrate; inset is the height profile along the white dashed line.

SUPPORTING INFORMATION

Screening of doping agents

As a general procedure, the screening of different dopant agents was carried out following the same synthetic protocol of **CNDs-2**, replacing 1,4-benzoquinone with 2,3-dimethoxy-5-methyl-1,4-benzoquinone, 1,4-naphthoquinone or terephthalaldehyde.

Table S1. Mass and g_{abs} values obtained upon the addition of a dopant different from 1,4- benzoquinone.

Modified dopant	mmol/mass added	g_{abs} *(10^{-4})	Solid color	mass (mg)
None	0.264 mmol/28.5 mg	4.6 (λ=417 nm)	brown	41
2,3-dimethoxy-5-methyl-1,4-benzoquinone	0.264 mmol/48 mg	-6.8 (λ=291 nm)	brown	27
1,4-naphthoquinone	0.264 mmol/41.7 mg	-2.3 (λ=285 nm)	brown	11
Terephthalaldehyde [a)]	0.264 mmol/28 mg	5.4 (λ=291 nm)	yellow	54

[a)] This reaction was carried out using (*R*)-1,1′-binaphthyl-2,2′-diamine, the others with (*S*)-1,1′-binaphthyl-2,2′-diamine.

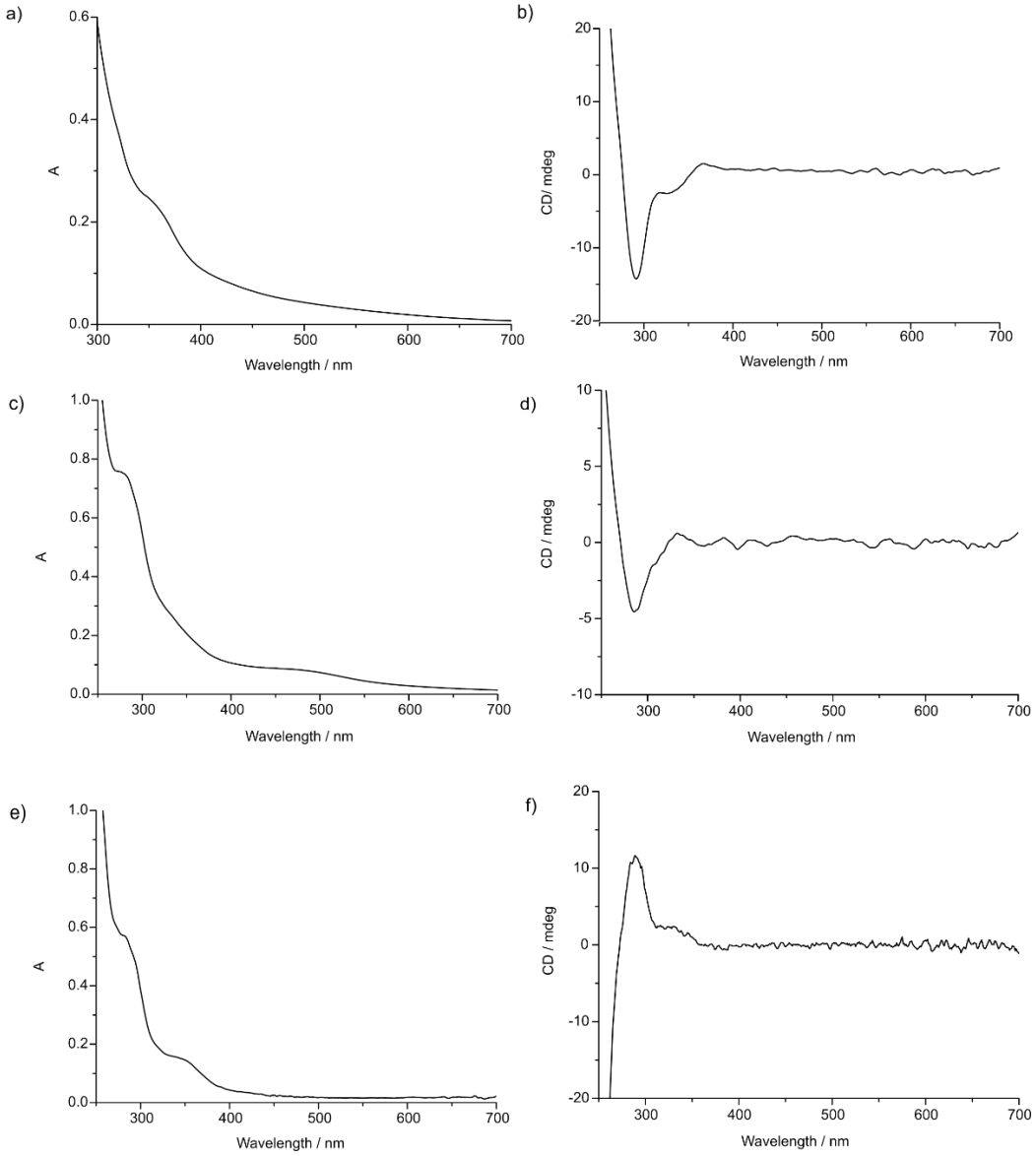

Figure S7. UV-Vis and ECD spectra of Carbon Nanodots from 2,3-dimethoxy-5-methyl-1,4-benzoquinone (a. and b.), 1,4-naphthoquinone (c. and d.) and terephthalaldehyde (e. and f.). Spectra recorded in $CHCl_3$.

SUPPORTING INFORMATION

Survey of synthetic parameters

As a general procedure, citric acid (76 mg, 0.396 mmol, 1.5 eq), (*S*)-1,1′-binaphthyl-2,2′-diamine (75 mg, 0.264 mmol, 1 eq.) and benzoquinone (28.5 mg, 0.264 mmol, 1 eq.) and were dissolved in N,N-dimethylformamide (DMF) (250 µL) and then reacted at 240°C, 200 W for 300 seconds. In the process of microwave heating, the solution changes color from burgundy to dark brown as a result of formation of CNDs. The solution was diluted with DMF and filtered through a 0.1 µm microporous membrane to remove possible large aggregates. The solution was collected and 50 mL of cold diethyl ether (Et_2O) were added in order to induce CNDs' precipitation. The precipitate was filtered through a 0.1 µm microporous membrane and washed with 50 mL of Et_2O, giving a brown solids. In the case of entry (E), microwave power was set at 300 W in order to reach a higher temperature.

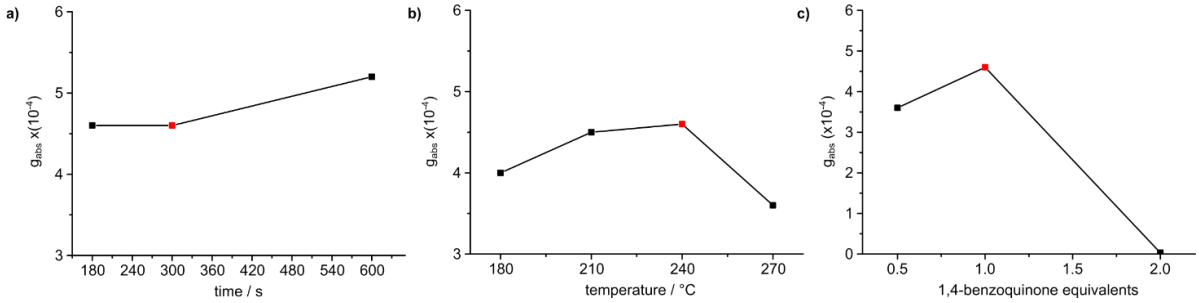

Figure S8. Trend of the g_{abs} calculated at 417 nm in function of (a) time, (b) temperature and (c) equivalents of 1,4-benzoquinone. Red squares indicate the standard synthesis conditions.

Table S2. Mass and g_{abs} values measured at 417 nm obtained upon modifying one synthetic parameter, either time, temperature or equivalents of 1,4-benzoquinone (BQ).

	Modified parameter	Value (unit)	g_{abs} *(10^{-4})	mass (mg)
	None	240 (°C), 200 (W), 300 (s)	4.6	41
A.	Time	180 (s)	4.6	40
B.	Time	600 (s)	5.2	43
C.	Temperature	180 (°C)	4.0	34
D.	Temperature	210 (°C)	4.5	32
E.	Temperature	270 (°C)	3.6	64
F.[a)]	Amount of BQ	0.5 (equiv.)	-3.6	24
G.	Amount of BQ	2.0 (equiv.)	0.03	65

[a)] This reaction was carried out using (*R*)-1,1′-binaphthyl-2,2′-diamine.

Size-Exclusion Chromatography analysis of CNDs-*S*-2

For Size-Exclusion Chromatography (SEC), a column packed with Sephadex LH-20 in N,N-dimethylformamide (DMF) operating at atmospheric pressure was employed. **CNDs-*S*-2** (19.4 mg) were dissolved in DMF (2 mL) and separated by SEC. Three fractions named SEC-fr1, SEC-fr2 and SEC-fr3 were obtained, according to their elution time. Finally, DMF was removed under reduced pressure, obtaining three oils. (SEC-fr1: 5.4 mg, SEC-fr2: 12.4 mg, SEC-fr3: 1.5 mg). All fractions display the typical excitation-dependent emission profile, with minor differences consistent with the presence of slightly different families of CNDs.[S1]

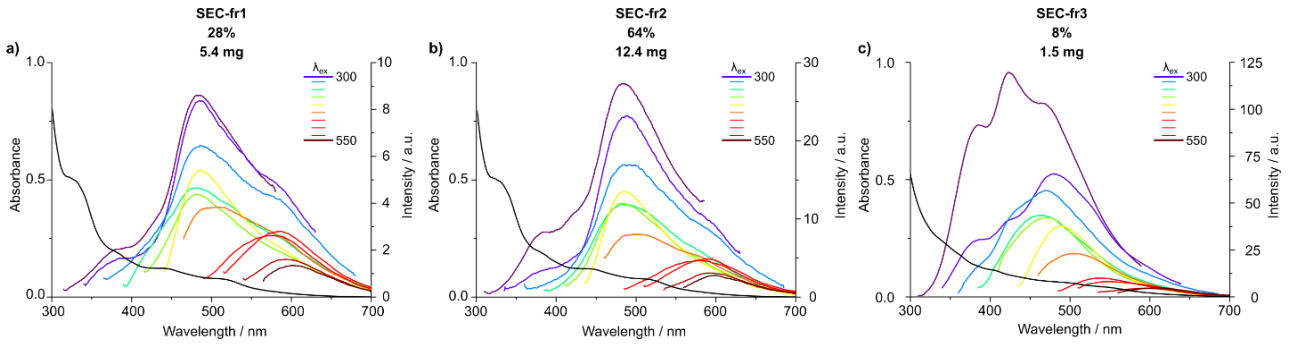

Figure S9. UV-Vis and fluorescence emission spectra of (a) SEC-fr1, (b) SEC-fr2 and (c) SEC-fr3 recorded at different excitation wavelengths. Experiments performed in $CHCl_3$ at r.t.

Morphological characterization of CNDs-*R*-2

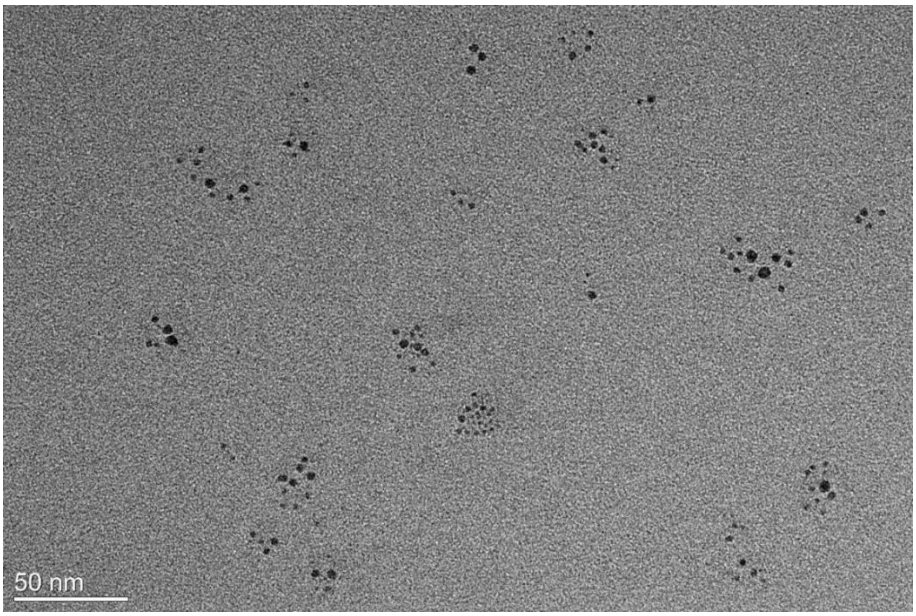

Figure S10. TEM image of **CNDs-*R*-2.**

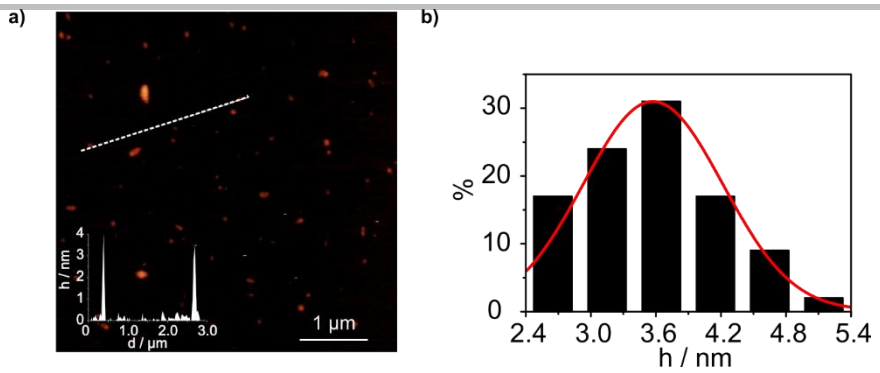

Figure S11. (a) Tapping mode AFM of **CNDs-*R*-2** deposited on a mica substrate; inset is the height profile along the white dashed line. (b) Size histogram of AFM height data, with distribution fit (red curve) based on a Gaussian distribution. **CNDs-*R*-2** possess a mean size of 3.57±0.64 nm, based on a statistic of 100 nanoparticles.

X-Ray Photoelectron Spectroscopy of CNDs-2

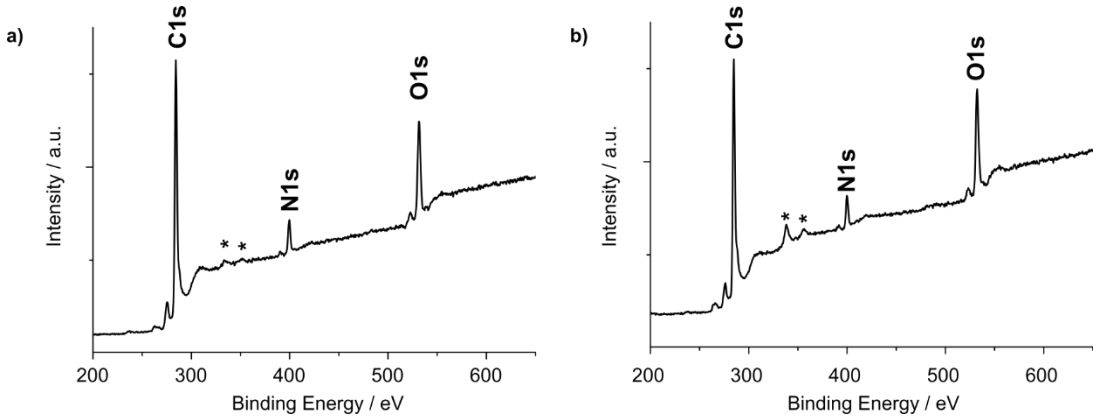

Figure S12. XPS survey of (a) **CNDs-*R*-2** and (b) **CNDs-*S*-2**, showing the C1s, N1s and O1s peaks (* from gold substrate Au4d3, Au4d5 and Au4p).

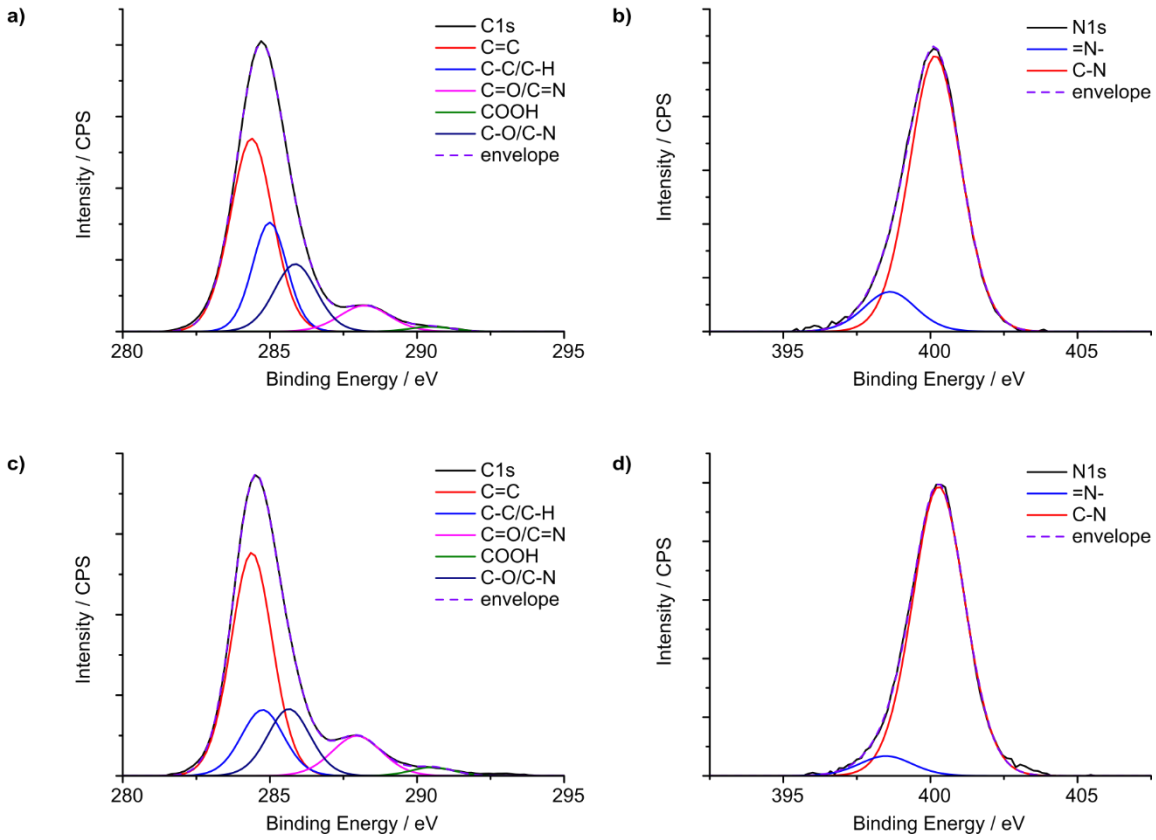

Figure S13. (a,b) Deconvoluted C1s and N1s spectra of **CNDs-*R*-2**; (c,d) deconvoluted C1s and N1s spectra of **CNDs-*S*-2**.

Table S3. XPS percentage of C, N, and O atoms and their deconvoluted components in **CNDs-*R*-2** and **CNDs-*S*-2** as determined by XPS measurements.

	CNDs-*R*-2	**CNDs-*S*-2**
C%	**81.9**	**80.0**
C=C	50.3	53.5
C-C/C-H	23.0	16.3
C=O/C=N	7.9	11.6
COOH	1.2	2.1
C-O/C-N	17.5	16.5
N%	**5.6**	**5.7**
=N-	12.6	6.4
C-N	87.4	93.6
O%	**12.5**	**14.3**

X-Ray Photoelectron Spectroscopy of CNDs-1

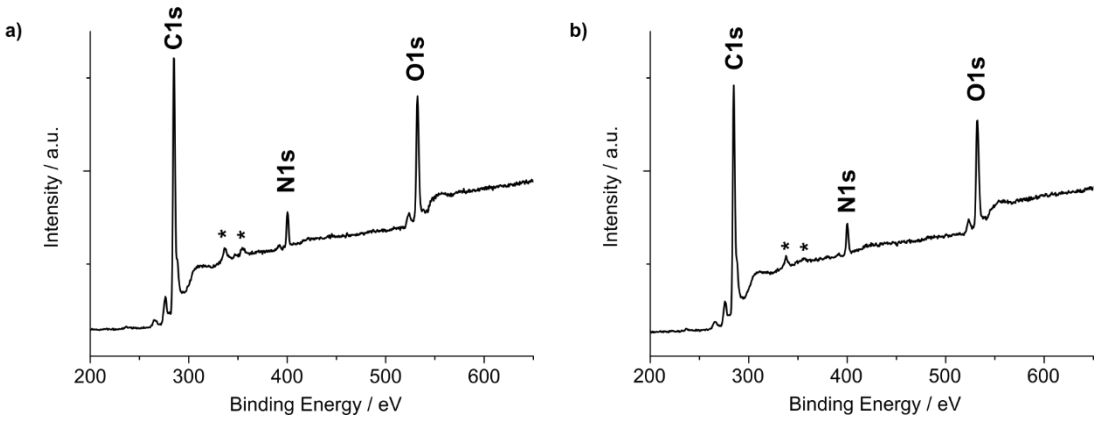

Figure S14. XPS survey of (a) **CNDs-*R*-1**, (b) **CNDs-*S*-1** showing the C1s, N1s and O1s peaks (* from gold substrate Au4d3, Au4d5 and Au4p).

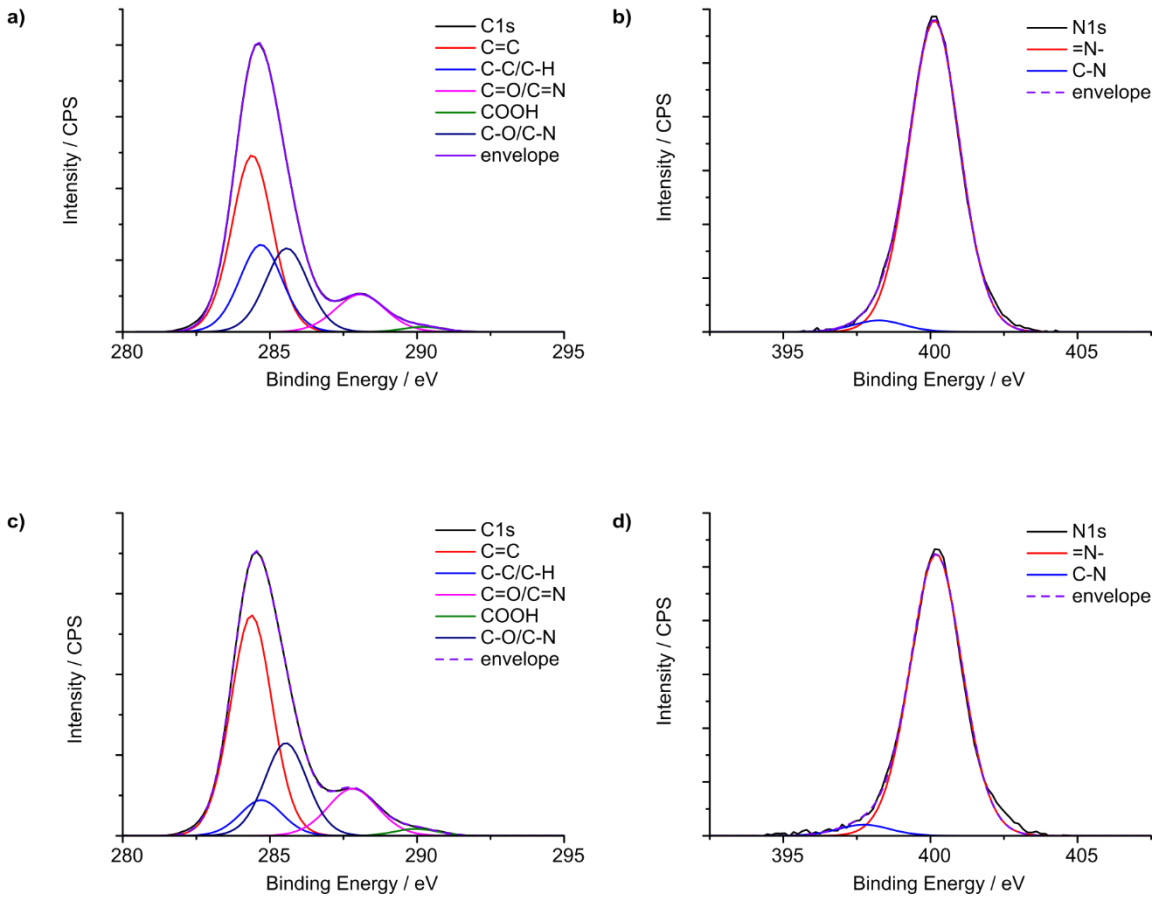

Figure S15. (a,b) Deconvoluted C1s and N1s spectra of **CNDs-*R*-1**; (c,d) deconvoluted C1s and N1s spectra of **CNDs-*S*-1**.

Table S4. XPS percentage of C, N, and O atoms and their deconvoluted components in **CNDs-*R*-1** and **CNDs-*S*-1**, as determined by XPS measurements.

	CNDs-*R*-1	**CNDs-*S*-1**
C%	**80.4**	**80.4**
C=C	43.5	52.9
C-C/C-H	22.4	8.8
C=O/C=N	11.4	13.7
COOH	1.2	1.7
C-O/C-N	21.5	22.9
N%	**5.3**	**5.6**
=N-	96.4	96.3
C-N	3.6	3.7
O%	**14.3**	**14.0**

Fourier-Transform Infrared Spectroscopy characterization

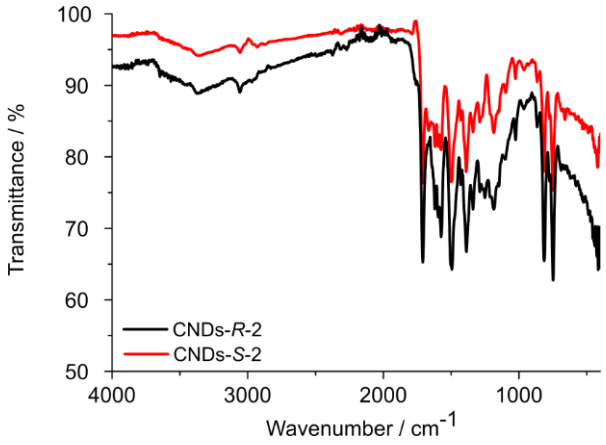

Figure S16. ATR-FTIR spectra of **CNDs-*R*-2** (black line) and **CNDs-*S*-2** (red line).

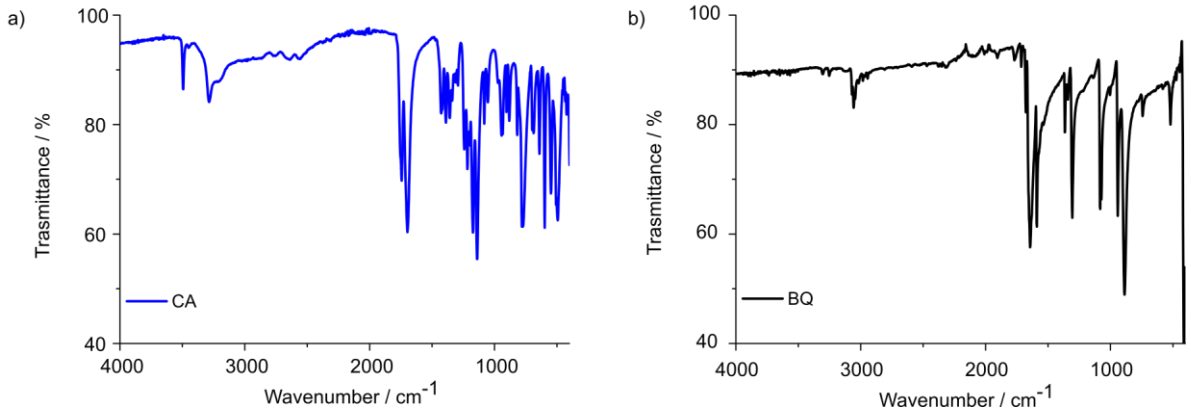

Figure S17: ATR-FTIR spectra of molecular precursors (a) citric acid and (b) 1,4-benzoquinone**.**

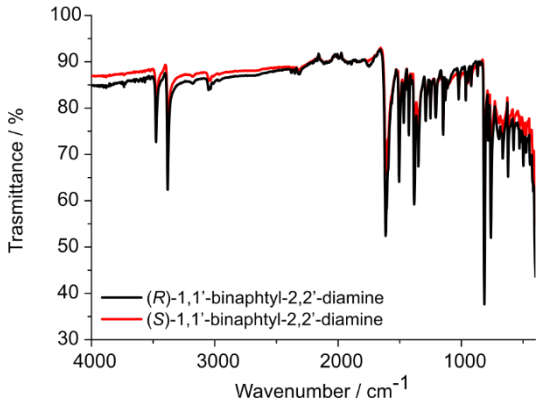

Figure S18: ATR-FTIR spectra of *R*- (black line) and *S*-1,1'-binaphtyl-2,2'-diamine (red line).

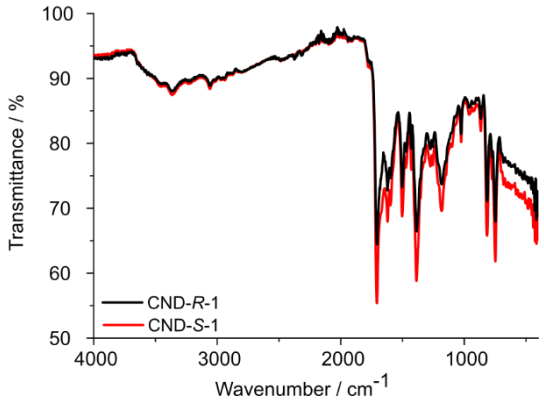

Figure S19: ATR-FTIR spectra of **CND-*R*-1** (black line) and **CND-*S*-1** (red line).

Structural characterization of CNDs-*R*-2

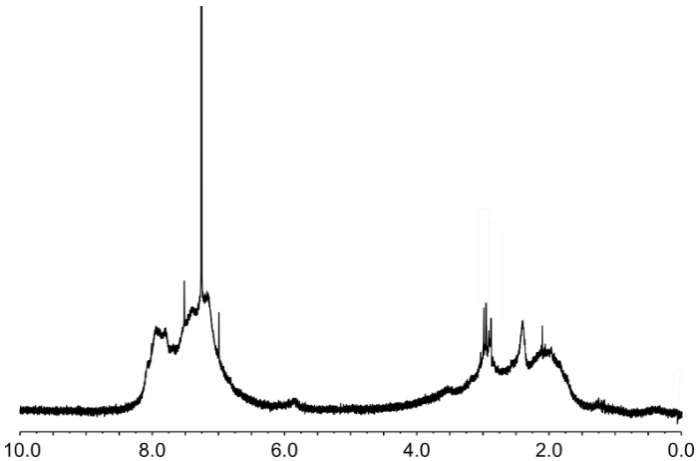

Figure S20. ^{1}H-NMR ($CDCl_3$, 400 MHz, r.t.) of **CNDs-*R*-2.**

Photophysical characterization of *CNDs-2* in multiple solvents

Table S5. Values of g_{abs}, λ_{em}, and τ_{ave} obtained for **CNDs-2** in different solvents. Polarity indexes E^N_T are taken from ref. [4].

Solvent	E_T^N	$\lvert g_{abs} \rvert$ (×10^{-4})	λ_{em}	τ_{ave}
$CHCl_3$	0.259	4.6	480	2.09
DCM	0.309	4.9	484	2.60
DMF	0.386	6.0	479	2.58
DMSO	0.444	5.8	482	3.04
EtOH	0.654	6.0	484	1.71

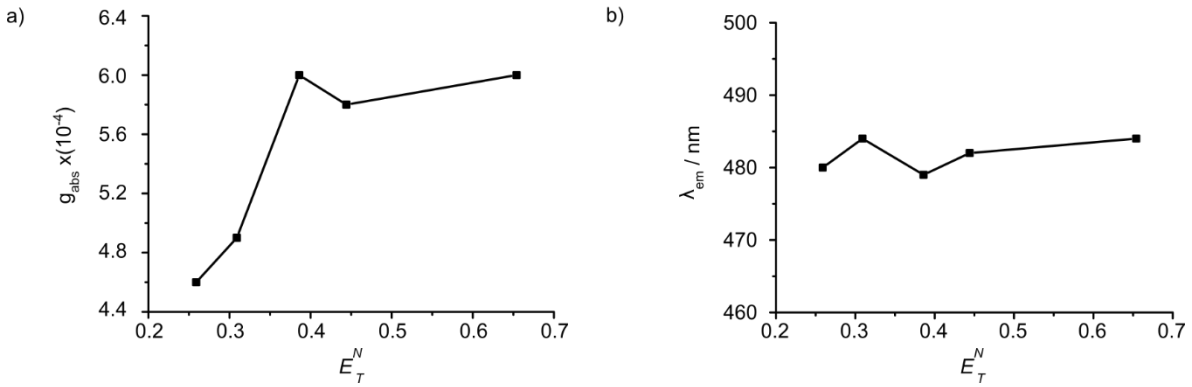

Figure S21: Plots of g_{abs} (at 417 nm) *vs* E_T^N (left) and λ_{em}^{max} *vs* E_T^N (right).

Optical characterization of CNDs-*R*-2

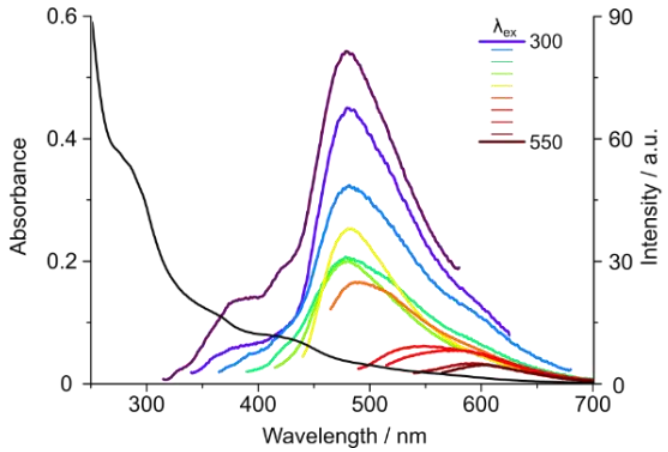

Figure S22. UV-Vis and fluorescence emission spectra of **CNDs-*R*-2** recorded at different excitation wavelengths. Experiments were performed in $CHCl_3$ at r.t. at concentrations between 0.05 and 0.01 mg/mL.

SUPPORTING INFORMATION

Chiroptical characterization of *R*- and *S*-1,1'-binaphthyl-2,2'-diamine

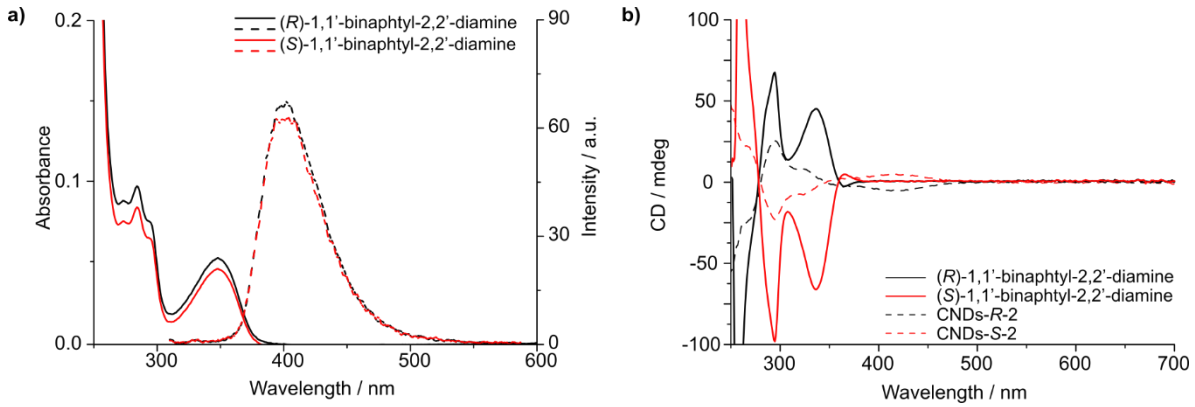

Figure S23. (a) UV-Vis spectra (solid lines) and fluorescence emission spectra (dashed lines) of (*R*)- (black line) and (*S*)-1,1′-binaphthyl-2,2′-diamine (red line). Fluorescence emission spectra are recorded at λ_{ex}=300 nm, with a maximum peak at λ_{em}=400 nm. (b) ECD spectra of (*R*)- (black solid line) and (*S*)-1,1′-binaphthyl-2,2′-diamine (red solid line). As reference, ECD spectra of **CNDs-*R*-2** (black dashed line) and **CNDs-*S*-2** (red dashed line) are reported. Experiments performed in $CHCl_3$ at r.t..

Quantum Yield meaurements of CNDs-2

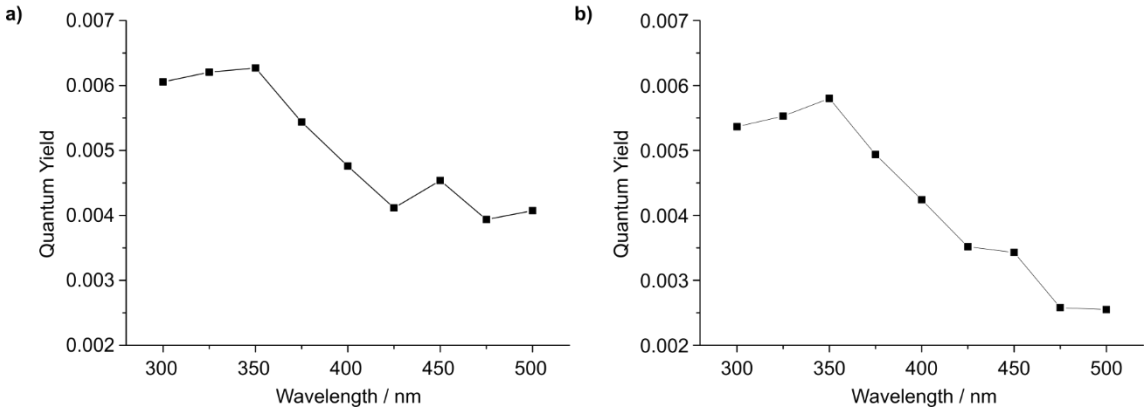

Figure S24. Quantum yield of (a) **CNDs-*S*-2** and (b) **CNDs-*R*-2** measured upon changing the excitation wavelength.

g_{lum} measurements of CNDs-2

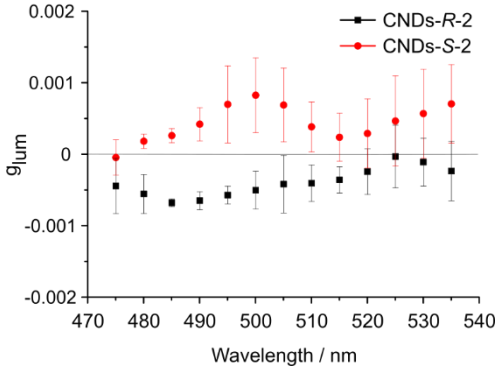

Figure S25. g_{lum} of **CNDs-*R*-2** (black circle points) and **CNDs-*S*-2** (red circle points) *vs* wavelength. Note that g_{lum} is noisy on the spectral edges where emission intensity becomes vanishing small.

Circularly Polarized Luminescence of CNDs-2 in DMF

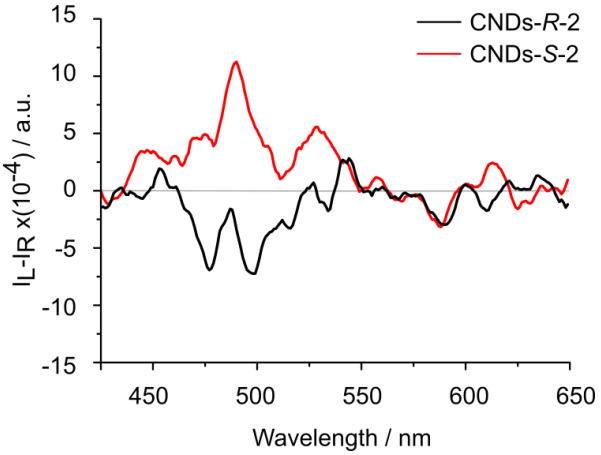

Figure S26. CPL spectra of **CNDs-*R*-2** (black line) and **CNDs-*S*-2** (red line) in DMF, excited at 365 nm.

Synthesis of Carbon Nanodots in absence of chiral diamine (CNDs-BQ)

Citric acid (76 mg, 0.396 mmol, 1.5 eq) and benzoquinone (28.5 mg, 0.264 mmol, 1 eq.) were dissolved in N,N-dimethylformamide (DMF) (250 µL) and then heated at 240°C, 200 W for 300 seconds. In the process of microwave heating, the solution changes color from yellow to brown as a result of formation of CNDs. The solution was diluted with DMF and filtered through a 0.1 µm microporous membrane to remove possible large aggregates. The solution was collected and 50 mL of cold diethyl ether (Et_2O) were added in order to induce CNDs' precipitation. The precipitate was filtered through a 0.1 µm microporous membrane and washed with 50 mL of Et_2O, giving a black solid (11 mg). Due to poor solubility of **CNDs-BQ** in $CHCl_3$, the optical characterization was performed in DMSO.

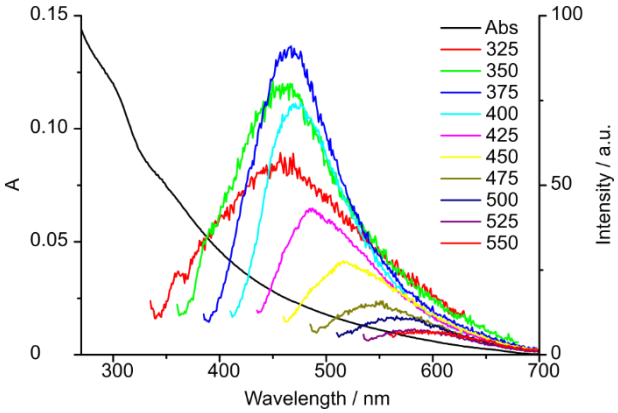

Figure S27. UV-Vis absorption and emission spectra of **CNDs-BQ** recorded in DMSO. The excitation wavelengths are shown inside the figure.

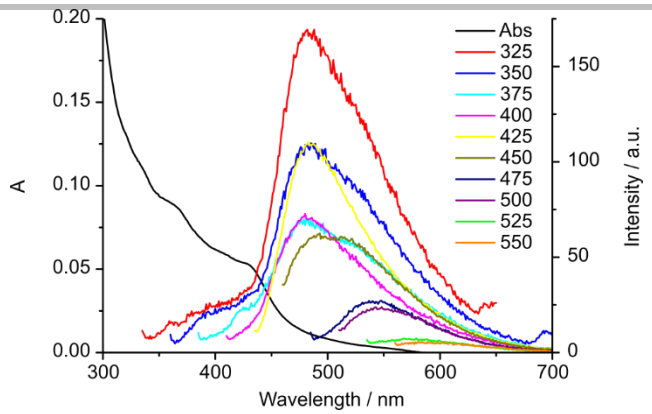

Figure S28. UV-Vis absorption and emission spectra of **CNDs-*S*** recorded in DMSO. The excitation wavelengths are shown inside the figure.

Circularly Polarized Luminescence of *R*- and *S*-1,1'-binaphthyl-2,2'-diamine

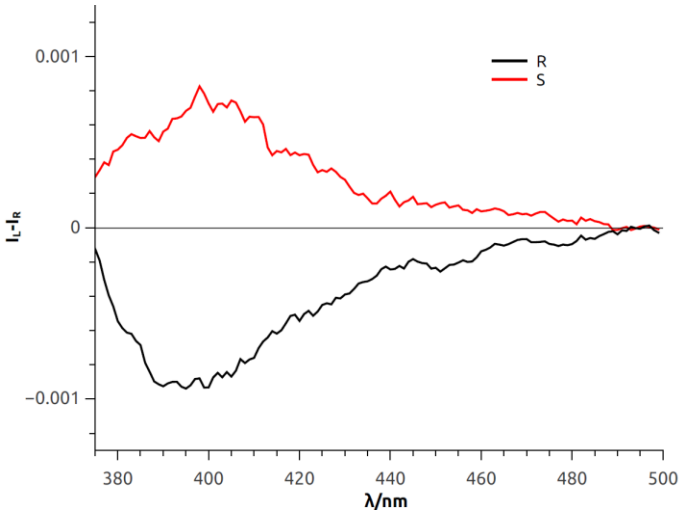

Figure S29. CPL spectra of (*R*)- (black line) and (*S*)-1,1′-binaphthyl-2,2′-diamine (red line) in CH_2Cl_2, excited at 365 nm.

Thermogravimetric analysis of CNDs-*R*-2

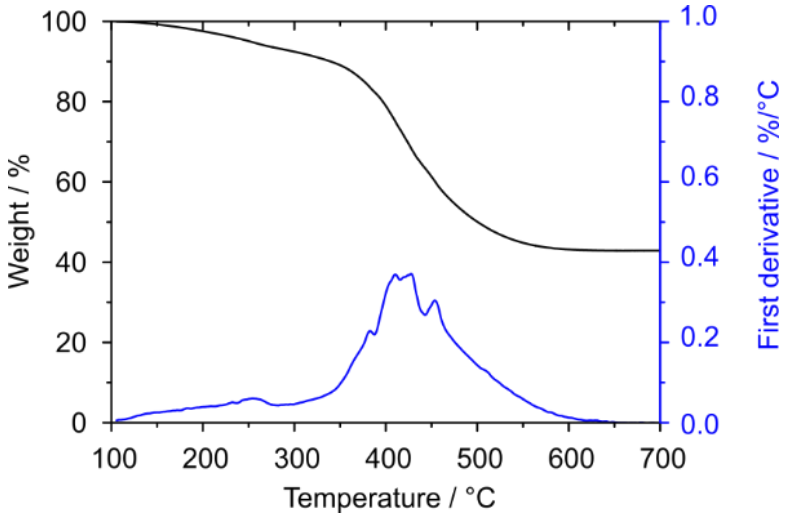

Figure S30. Thermogravimetric analysis of **CNDs-*R*-2** (black line) and its first derivative (blue line).

Lifetime measurements of CNDs-2

In both figures, the yellow curve corresponds to the sample fluorescence decay, the blue curve corresponds to the Instrument Response function – used to fit the fluorescence decays – and the magenta curve corresponds to the best fit, with their respective residuals (green line).

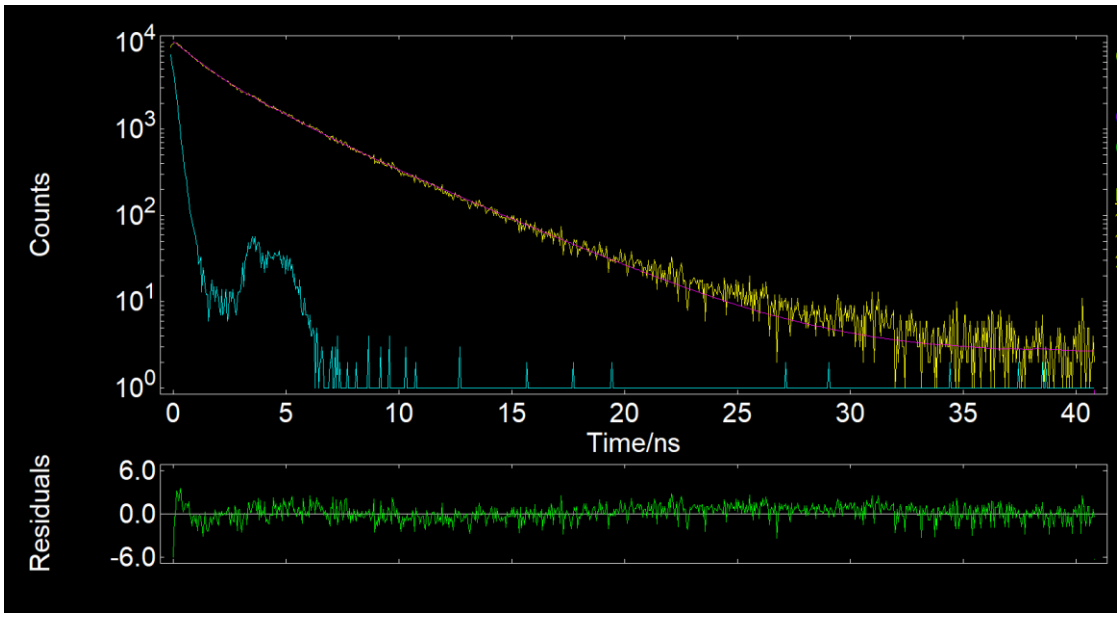

Figure S31. Fluorescence decay curve of **CNDs-*R*-2** in CH_2Cl_2 (λ_{exc} = 375 nm, λ_{em} = 490 nm).

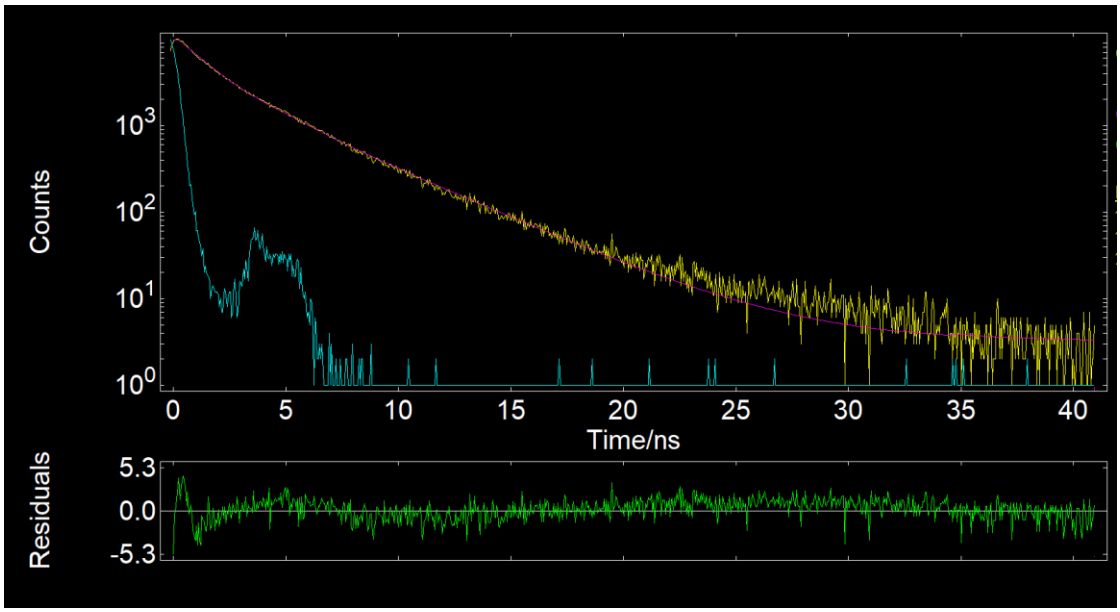

Figure S32. Fluorescence decay curve of **CNDs-*S*-2** in CH_2Cl_2 (λ_{exc} = 375 nm, λ_{em} = 490 nm).

Table S6. Fitting parameters of the fluorescence decay curves.

Sample	A_1	$\tau_1 \pm 0.1$ (ns)	A_2	$\tau_2 \pm 0.1$ (ns)	τ_{ave} (ns)
CNDs-*R*-2	0.07	1.51	0.03	3.86	2.74
CNDs-*S*-2	0.07	1.36	0.03	3.86	2.73

SUPPORTING INFORMATION

References

[1] F. Arcudi, L. Dordevic, M. Prato, Angew. Chem. Int. Ed. 2016, 55 (6), 2107–2112.
[2] F. Zinna, T. Bruhn, C. A. Guido, J. Ahrens, M. Bröring, L. Di Bari, G. Pescitelli, Chem. Eur. J. 2016, 22, 16089-16098.
[3] T. Kinuta, N. Tajima, M. Fujiki, M. Miyazawa, Y. Imai, Tetrahedron 2012, 68, 4791-4796.
[4] C. Reicherd, Chem. Rev. 1994, 94, 2319-2358

Author Contributions

Investigation
SDN Lead, FA Equal, FZ Equal, GR Support

Validation
GR Lead, MP Lead, FZ Lead, LDB Lead

Writing original
GR Lead, FZ Lead, SDN Lead

Writing review and editing
MP Lead, LDB Lead, FA Support

Funding
LDB Lead, MP Lead